A PREDICTIVE MODEL FOR THE CUTTING FORCE IN WOOD MACHINING DEVELOPED USING MECHANICAL PROPERTIES

Andrew Naylor,[a,*] Phil Hackney,[a] Noel Perera,[a] and Emil Clahr [b]

In this study a number of work-piece variations were evaluated whilst limiting the cutting conditions. Eight wood species controlled at four moisture levels were machined along and across the wood grain. The tool used during cutting was designed to resemble a rip saw tooth with zero rake angle and narrow edge width. Each work-piece variation machined in the cutting tests was subjected to mechanical tests that evaluated bending properties across the grain and shear properties along the grain. The regression model establishes a relationship between the bending properties for cutting forces across the grain, as well as shear properties for cutting forces along the grain. F and R^2 values show that the elastic properties of the wood in bending and shear have less influence on the cutting forces when compared to the strength and toughness. Additionally, density is seen to have less influence on the cutting force along the grain. This is explained by the tool passing through an unquantifiable proportion of early and latewood fibers from the annual growth rings. Cutting across the grain, the tool is forced to machine through approximately the same proportion of earlywood and latewood fibres.

Keywords: Wood machining; Manual wood sawing; Mechanical testing; Regression modeling

Contact information: a: School of Computing, Engineering and Information Sciences, Ellison Building, Northumbria University, Newcastle Upon Tyne, NE1 8ST, United Kingdom; b: Research and Development Centre for Wood Working, SNA Europe, Box 1103 82113 Bollnäs, Sweden
**Corresponding author: andrew2.naylor@northumbria.ac.uk*

INTRODUCTION

Fundamental wood machining research typically uses characterized chip formation, coupled with tool forces in order to explain the cutting mechanics. Franz (1955; 1958) characterized chip formation along the grain (90° to 0°) with varied rake angles and edge radii, concluding that although all chip types observed have very different characteristics, the primary cutting mechanics machining in this direction is shearing. Woodson and Koch (1970) evaluated the chip formation across the grain (0° to 90°) by means of a veneer peeling case study. They concluded that the chip is formed by an initial tear caused by compression, followed by an ongoing shearing process with some tensile failure. McKenzie (1961) studied the cutting mechanics machining the wood end grain (90° to 90°) with the observation that the chip is formed by a tensile failure mode, causing parallel gaps to propagate between the wood fibers. All of these studies implemented the use of planning tools, removing wood across the entire width of the work-piece. Furthermore, none of these studies have thoroughly investigated the influence of mechanical properties on tool forces.

More recent research (Axelsson *et al*. 1991; Cristovao *et al*. 2011) looks at the effects of moisture content and density on tool forces. In these studies the density is measured by taking grayscale images of the internal wood structure using CT scanning. Additionally, wood fracture mechanics during sawing has been investigated (Orlowski *et al*. 2009, 2011). Loehnertz and Cooz (1998) recorded saw tooth cutting, thrust, and side forces for many hardwood species. This study focused on the machining the wood end grain (sawmill applications) for dry and saturated work-pieces. Eyma *et al*. (2004, 2005) used density and hardness combined with mechanical properties obtained parallel to the grain such as: shear stress, compressive stress, elastic modulus, and toughness to develop cutting force relationships.

Published work (Naylor *et al*. 2011) details the findings of cutting tests performed in the test rig described in the methodology. Optical microscope images of the chip formed cutting along the grain are comparable to the chip formation types characterized by Franz (1955, 1958). Dry work-pieces are noted to be the cause of the discontinuous and broken chips whilst work-pieces with higher moisture content are seen to yield the fuzzy chip types. The continuous chips are produced by machining wood at moisture content ranging from 10 to 20%. Observed surface formation cutting across the grain does not bear any resemblance to the chip observed by Woodson and Koch (1970); instead, a bending of the wood fibers perpendicular to the grain is seen. Furthermore, it is observed that increased moisture content leads to an increase in elasticity, causing the fibers to spring back and cover the machined tool path.

The existing body of work often has a limited consideration for the effects of multiple mechanical properties on the tool forces. Furthermore, often only one wood grain direction and/or species is selected as the work-piece. In this study, properties obtained using a longitudinal shear methodology was used as parameters for predicting cutting force along the grain. Properties obtained via a three-point bending test methodology were used as parameters for predicting cutting force across the grain. Multiple wood species and moisture levels were used.

EXPERIMENTAL METHODOLOGY

The experimental test rig comprised of a cutting tool driven by a 3-axis CNC router machine. The tool was rigidly attached to the actuating arm of the router machine and was driven at a single speed of 100 mm/s for each cut performed. The work-piece was mounted on a force dynamometer equipped with piezoelectric load cells that measured the cutting, thrust, and side force components acting on the tool. Only the cutting and thrust force components were taken into consideration for this analysis. The test rig schematic diagram (Fig. 1) details the set-up of the data acquisition system. To obtain tool force data, the cutting tool **(1)** was used to machine through the work-piece attached to the force dynamometer **(2)**. The three piezoelectric transducers in the dynamometer each generated a charge in response to the cutting forces (3.9 pC/1 N in X and Y directions, 1.95 pC/1 N in the Z direction). These signals fed into the charge amplifier **(3),** where the signals were calibrated for a 10V input to the data acquisition PLC **(4)** (3900 pC/10 V in X and Y directions, 1950 pC/10 V in Z direction: Hence 1 N =

0.01 V). The PLC converted the signals from analogue to digital, and the data was then analysed using LabView signal express software **(5)**.

The high speed steel tool used in the experiment has geometry similar to the hand-saw rip tooth formation (Fig. 2). The tool has an orthogonal cutting edge with a width of 1 mm and a rake angle (α) of zero. To ensure that the cutting edge was sharp, the tool was sharpened using precision grinding equipment prior to performing the test runs. The two machining directions selected for the experiment were 90° to 0° (along the grain) and 0° to 90° (across the grain) as these are deemed to be the most common directions for manual wood sawing. This is specifically relevant to the scope of this author's research into the performance of individual handsaw teeth. Machining was performed along and across the radial wood plane rather than the tangential. This is because the ratio of earlywood to latewood bands on the radial plane is approximately 1:1; it was expected that the tool would pass through both earlywood and latewood fibres. Eight species of wood were evaluated in the experiment: five softwoods (Scots pine, yellow pine, Siberian larch, Douglas fir, and western red cedar) and three hardwoods (ash, beech, and sapele). Each of these wood species had four separate moisture levels: DRY (≈6%), 10%, 20%, and SATURATED (>30%). Including the two machining directions, this amounts to 64 work-piece variables. Each of the 64 work-piece variations were machined at three cut depths: 0.4, 0.8, and 1.2 mm, providing a total of 192 cutting force values for analysis.

Moisture content was determined electronically using a hand held protimeter. An average was taken of a minimum of six measurements from the radial plane of each wood work-piece at a minimum depth of 5 mm. Density was determined through manual measurements of the work-piece using a digital vernier calliper combined with measurement of the mass using calibrated electronic scales. A minimum of six depth and breadth measurements were taken from various positions for a specified work-piece length. The average depth, breadth, and length were used to estimate the volume of the work-piece. The general equation: $\boldsymbol{\rho = m/v}$ (kg/m^3), was used to determine the final density value.

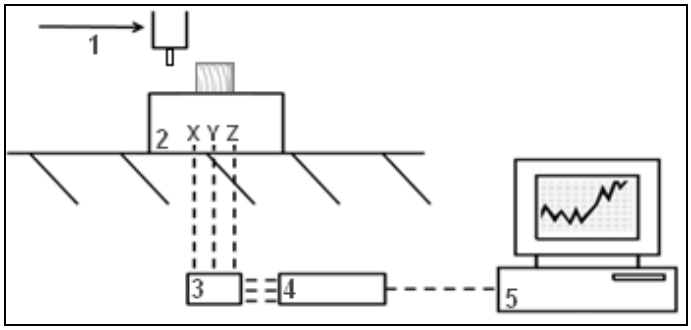

Fig. 1. Test rig schematic diagram

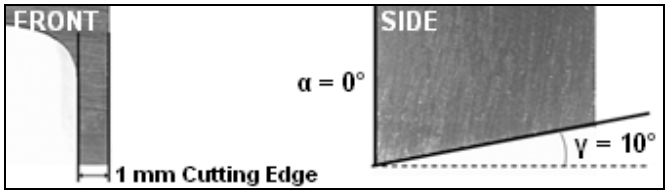

Fig. 2. Optical microscope images of the cutting tool

Only clear specimens of each selected wood species were used as test samples for mechanical testing. This was to eliminate the detrimental effects of knots or distorted grain on the obtained results. A total of 32 work-piece variations were evaluated for each mechanical test. This was based upon the eight wood species and four moisture variations. No repeats were performed for any given variation however the test sequence was randomised to eliminate any systematic error.

ASTM D143-09 (2009) standard test procedures for longitudinal shear (Fig. 3) and three-point bending (Fig. 4) were carried out in a universal testing machine to characterize wood strength across and along the grain, respectively. The longitudinal shear specimen is placed between the crosshead of the testing machine and an anvil allowing the wood to shear parallel to the grain direction. A 0.6 mm/min crosshead speed was maintained throughout testing until failure. Derived shear stress and strain, Eq.1 and Eq.2 respectively, are noted. The span (L) of the three-point bending specimens was limited to 300 mm with a 20 mm depth (d); this is in keeping with the specified 14:1 minimum span to depth ratio. An additional criterion that was also specified by the standard was a 1.3 mm/min crosshead maintained throughout testing until failure. Derived bending stress and strain, Eq.3 and Eq.4 respectively, are also noted.

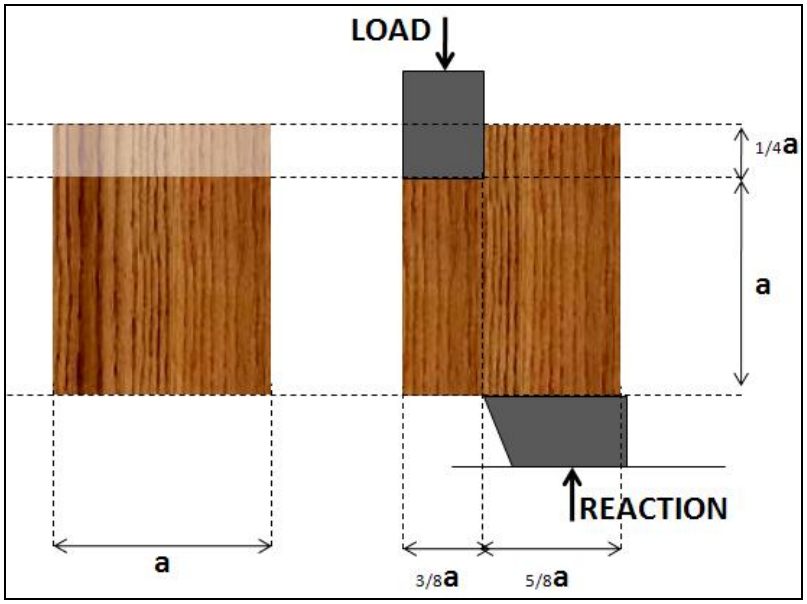

Fig. 3. Methodology for wood longitudinal shear test

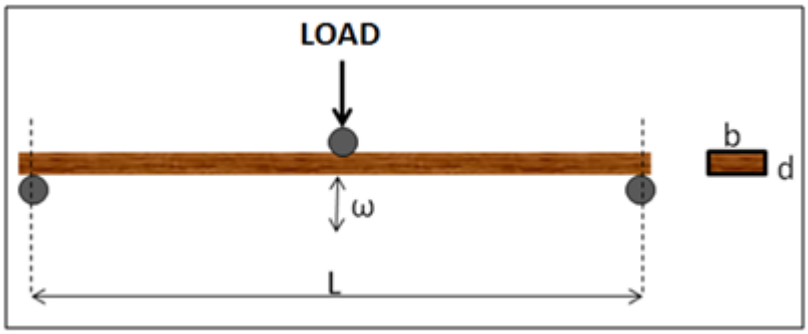

Fig. 4. Methodology for wood three-point bending test

Measurements of recorded Force (**F**) vs. Displacement (**ω**) were taken by the universal testing machine. Each **F** vs. **ω** plot was easily converted to a Stress vs. Strain plot, with the curve taking the form of a quadratic polynomial. The gradient of the plot in the linear elastic region provided the modulus of elasticity (**MOE**) for bending and the shear modulus (**G**). Likewise the modulus of rupture (**MOR**) for bending and the shear strength (**τ**) were taken as the stress at point of fracture. Toughness (**U**) was obtained by taking a definite integral of the function between zero and point of fracture (**n**) (Eq. 5).

The prepared wood specimens for the three point bending tests, longitudinal shear tests, and controlled cutting tests were carefully cut from the same one meter length of timber. This was to ensure that the mechanical properties and cutting forces obtained were for near identical work-pieces. In summary, the observed response taken from the cutting tests was the tool force in the direction of cutting. The controlled variables were machining direction, moisture content (**MC**), and depth of cut (**δ**) with the measured variables of mechanical properties and density (**ρ**). Each work-piece was machined along and across the grain, disregarding the wood end-grain direction. The model parameters acted as predictors for two separate models cutting along and across the grain.

$$\gamma = \frac{\omega}{3/8\, a} \tag{1}$$

$$\tau = \frac{F}{a^2} \tag{2}$$

$$\sigma = \frac{3FL}{2bd^2} \tag{3}$$

$$\varepsilon = \frac{6\omega d}{L^2} \tag{4}$$

$$U = \int_n^0 f(\varepsilon) = \int_n^0 a\varepsilon^2 + b\varepsilon + c \tag{5}$$

STATISTICAL METHODS

Multiple least squares method was used to develop the regression models based upon several categorical predictors. In both cases, force in the direction of cutting, **Fc** (N), was the measured response with **MOE**, **MOR**, **ρ**, **Ub**, **MC**, and **δ** as predictors for the model across the grain and **G**, **τ, ρ**, **Us**, **MC**, and **δ** as predictors for the model along the grain (Table 1).

Simple least squares method was subsequently used to weight the effects of the obtained mechanical properties on the cutting force. Specific cutting force (**Fsp**) defined as force over depth of cut was used as the response value for the selected categorical predictors. Across the grain these predictors are: **MOE**, **MOR**, **ρ**, and **Kb**. Along the

grain the predictors are; **G**, **τ**, **ρ**, and **Ks**. Moisture content was not selected for these trials in order to keep an emphasis on the properties obtained through mechanical testing. The **F** and $\mathbf{R^2}$ values were used to quantify the influence of the obtained mechanical properties on the predicted cutting force (Eq. 6 and Eq. 7).

Table 1. Categorical Predictors Used for Regression Models

Symbol	*Description*	*Units*
MOR	Bending strength across the grain	MPa
τ	Shear strength along the grain	MPa
MOE	Bending elastic modulus across the grain	MPa
G	Shear elastic modulus along the grain	MPa
Ub	Bending toughness across the grain	J/m^2
Us	Shear toughness along the grain	J/m^2
MC	Moisture content	%
δ	Depth of cut	mm

$$\text{F Value} = \frac{\text{explained variance}}{\text{unexplained variance}} = \frac{MS_{REG}}{MS_{RES}} \quad (6)$$

$$R^2 = \frac{SS_{REG}}{(SS_{REG} + SS_{RES})} \quad (7)$$

RESULTS

Mechanical Properties

For all moisture levels evaluated, the mean values for **MOR** range from 50 to 90 MPa. A linear decrease was observed for increased moisture content, with the highest values yielded by the three hardwood species tested, on average 70% greater than the softwood values. The mean values **MOE** ranged from 40000 to 80000 MPa, with a linear decrease observed for increased moisture content. There was no discernable pattern to suggest that the hardwoods yield higher **MOE** values than the softwoods. **Ub** on average ranged from 29000 to 50000 J/m^2. Once again a linear decrease in magnitude was observed for increased moisture content. The hardwoods yielded significantly higher values, on average 120% greater than the softwood values.

The mean **τ** values ranged from 5 to 12 MPa. The highest values represented the three hardwoods tested, which were approximately 45% greater than the softwoods. Furthermore a linear decrease in strength was observed with an increase in moisture content. The mean **G** values ranged from 15 to 230 MPa with the larger values once again representing the hardwoods. These values were approximately 50% greater than the softwoods. **G** was significantly influenced by moisture content with the average values obtained for the saturated work-pieces measuring only 6% the magnitude of the values obtained for the dry work-pieces. **Us** on average ranges from 18000 to 50000 J/m^2. Again a linear decrease in magnitude was observed for increased moisture content. In a similar

way to **Ub, Us** yielded significantly higher values for the three hardwood species tested, on average 150% greater than the softwood values.

Average values for **ρ** also showed a negative linear trend for increased moisture content. The hardwoods yield values approximately 45% greater in magnitude than the softwoods. For the nominal values of DRY (≈6%), 10%, and 20%; the measured moisture content values had a low standard deviation in proportion to the range. Furthermore the measured values did not deviate too far from the nominal values. The measured values for nominally SATURATED work-pieces have an average of 35% moisture content. The range and standard deviation are larger; this is due to the variation in wood fibre saturation for the different species.

Table.2. Obtained Mechanical Properties

	Species	MOE (MPa)	MOR (MPa)	Ub (J/m^2)	G (MPa)	τ (MPa)	Us (J/m^2)	ρ (kg/m^3)	MC (%)
DRY (NOMINAL)	Scots Pine	62800	79.21	33250	151.47	9.53	26650	576.64	6.00
	Yellow Pine	50800	47.72	24910	286.27	6.28	17100	484.80	6.00
	Douglas Fir	69200	72.01	49000	236.51	7.58	34080	496.62	8.00
	Western Red Cedar	91500	99.28	40600	52.78	8.62	31730	671.57	6.00
	Siberian Larch	73300	65.24	49020	260.16	9.31	54000	638.46	8.00
	Ash	57500	105.57	84000	277.03	17.06	94300	912.87	6.00
	Beech	88900	127.44	61750	363.83	15.55	86400	669.00	6.00
	Sapele	78000	92.73	58050	219.11	18.17	57200	819.08	6.00
	AVERAGE	**71500**	**86.15**	**50070**	**230.90**	**11.51**	**50180**	**658.63**	**6.50**
	RANGE	**40700**	**79.72**	**59090**	**311.05**	**11.89**	**77200**	**428.07**	**2.00**
	STANDARD DEVIATION	**14400**	**25.24**	**18350**	**94.06**	**4.65**	**28200**	**148.44**	**0.93**
10% (NOMINAL)	Scots Pine	58300	61.99	21000	152.64	7.97	25200	559.04	14.00
	Yellow Pine	40300	47.62	19200	91.30	5.69	16120	436.15	11.00
	Douglas Fir	61400	58.57	24750	43.32	3.97	26850	478.93	14.00
	Western Red Cedar	39500	54.60	22100	268.98	4.76	26250	460.96	11.00
	Siberian Larch	67000	88.62	28840	208.32	10.34	27280	615.38	11.00
	Ash	82300	119.09	61740	123.21	14.20	84000	850.73	10.00
	Beech	113600	95.04	47250	211.37	14.15	60750	696.65	11.00
	Sapele	91100	113.05	45500	691.02	14.31	28600	759.75	8.00
	AVERAGE	**69200**	**79.82**	**33790**	**223.77**	**9.42**	**36880**	**607.20**	**11.25**
	RANGE	**74100**	**71.47**	**42540**	**647.70**	**10.34**	**67880**	**414.58**	**6.00**
	STANDARD DEVIATION	**25400**	**27.77**	**15670**	**202.15**	**4.43**	**23080**	**151.22**	**1.98**
20% (NOMINAL)	Scots Pine	64900	53.85	8750	128.55	10.85	15260	546.36	20.00
	Yellow Pine	32400	30.57	3840	46.22	2.22	11700	416.88	25.00
	Douglas Fir	44700	40.92	20470	152.23	4.85	21000	462.60	25.00
	Western Red Cedar	46900	56.63	10330	138.98	3.74	16640	434.53	25.00
	Siberian Larch	40800	48.80	22500	136.96	5.76	24080	604.35	20.00
	Ash	77600	103.94	42750	84.88	7.32	70950	714.17	24.00
	Beech	51100	78.47	42000	209.07	7.17	35500	737.15	27.00
	Sapele	31500	62.47	38740	195.14	10.64	28250	632.64	23.00
	AVERAGE	**48700**	**59.46**	**23670**	**136.50**	**6.57**	**27920**	**568.59**	**23.63**
	RANGE	**46100**	**73.37**	**38910**	**162.85**	**8.63**	**59250**	**320.27**	**7.00**
	STANDARD DEVIATION	**15800**	**22.93**	**15730**	**53.23**	**3.08**	**18980**	**124.04**	**2.50**
SAT (NOMINAL)	Scots Pine	44100	47.00	15400	6.21	5.70	9100	530.23	32.00
	Yellow Pine	24900	26.65	10200	7.75	2.31	7100	407.70	35.00
	Douglas Fir	36600	29.69	22000	25.20	4.42	11600	448.67	35.00
	Western Red Cedar	43300	43.84	21930	19.91	3.49	11000	354.88	30.00
	Siberian Larch	44500	40.83	22800	7.71	4.71	14200	575.65	32.00
	Ash	56200	73.15	45990	18.45	6.34	40000	708.26	45.00
	Beech	58400	76.76	45600	16.20	8.35	31200	787.75	40.00
	Sapele	47800	69.15	45000	19.54	11.39	21000	595.21	31.00
	AVERAGE	**44500**	**50.88**	**28610**	**15.12**	**5.84**	**18150**	**551.04**	**35.00**
	RANGE	**33500**	**50.11**	**35790**	**18.99**	**9.08**	**32900**	**432.87**	**15.00**
	STANDARD DEVIATION	**10600**	**19.64**	**14610**	**7.02**	**2.89**	**11760**	**147.96**	**5.13**

Cutting Force Models

Force in the direction of cutting was used as the only measured response for the regression models. Measured thrust and side forces were negligible compared to the

cutting force. Multiple least squares method was used to develop the regression equations (Eq. 8 and Eq. 9), the regression plots shown with 95% prediction intervals (Fig. 5), and the residual histograms (Fig. 6). The models exhibited $\mathbf{R^2}$ values of 80% and 90% along and across the grain, respectively. Additionally, the ratio of range to standard deviation is considered (**R/SD**). These values evaluate the spread of the data and the variance. They were 4.54 and 4.66 along and across the grain, respectively.

The simple least squares method was used to quantify the influence of the obtained properties on the cutting force. The spread of the residual **Fsp** values had a data range of 159 N/mm across the grain and 168 N/mm along the grain. Standard deviation was also calculated with values of 34 across the grain and 33.5 along the grain. The ultimate material strength values yielded the highest $\mathbf{R^2}$ and **F** values with values for toughness following the same pattern (Fig. 7). The elastic properties yielded the lowest **F** and $\mathbf{R^2}$ values. Density, however, yielded very high **F** and $\mathbf{R^2}$ values across the grain with comparably low values along the grain.

Models excluding selected categorical predictors were also developed. Predicting the cutting force ($\mathbf{FC_P}$) along the grain by negating **G** returned an $\mathbf{R^2}$ value of 78.9%. Negating **ρ** along the grain returned an $\mathbf{R^2}$ value of 79.1%. Negating both **G** and **ρ** along the grain returned an $\mathbf{R^2}$ value of 78.6%. These only differ by a very small amount from the $\mathbf{R^2}$ value of 80% when all categorical predictors are used. Predicting the cutting force across the grain by negating **MOE** returns an $\mathbf{R^2}$ value of 85.9%, compared to the slightly larger value of 90% when using all categorical predictors. It is also noticed that the **F** values vary when using different combinations of categorical predictors. Along the grain, these vary from 59.33 using all of the categorical predictors, 67 excluding **G**, 68 excluding **ρ** and 84 excluding both **G** and **ρ**. When using all of the categorical predictors in the cutting force model across the grain, an **F** value of 90.54 is returned. By excluding **MOE** from this group of categorical predictors, a larger **F** value of 110 is returned.

Eq. 8. Regression equation along the Grain

$$\mathbf{FC_P} = -15.3 + 0.0243\,\mathbf{G} + 2.54\,\boldsymbol{\tau} - 0.0246\,\boldsymbol{\rho} + 65.4\,\boldsymbol{\delta} - 0.301\,\mathbf{MC} + 0.00492\,\mathbf{Us}$$

$\mathbf{R^2} = 0.8$ **Range** = 155.7 **SD** = 34.29

Eq. 9. Regression equation across the Grain

$$\mathbf{FC_P} = -72.7 - 0.000093\,\mathbf{MOE} + 0.235\,\mathbf{MOR} + 0.0594\,\boldsymbol{\rho} + 108\,\boldsymbol{\delta} - 0.129\,\mathbf{MC} + 0.00526\,\mathbf{Ub}$$

$\mathbf{R^2} = 0.9$ **Range** = 210.4 **SD** = 45.12

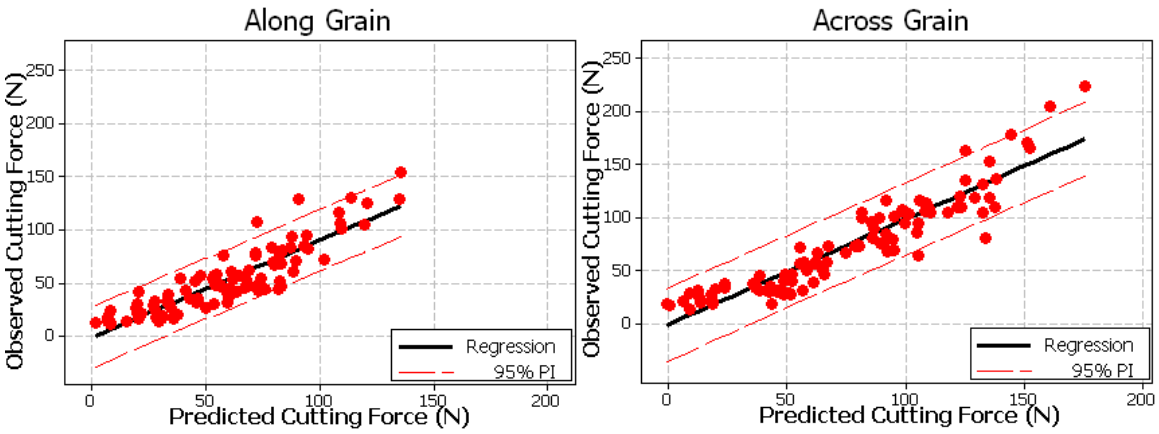

Fig. 5. Regression plots for cutting along and across the wood grain

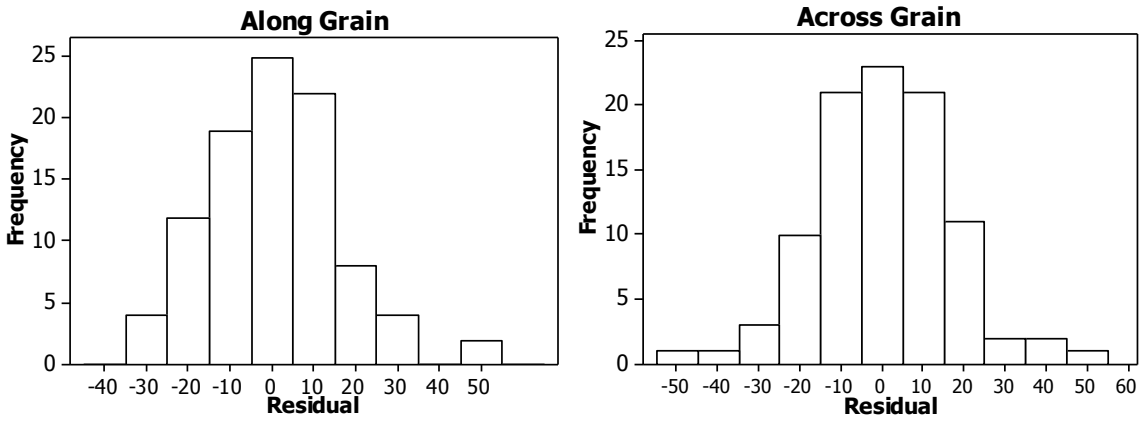

Fig. 6. Residual histogram plots of predictive models for cutting along and across the wood grain

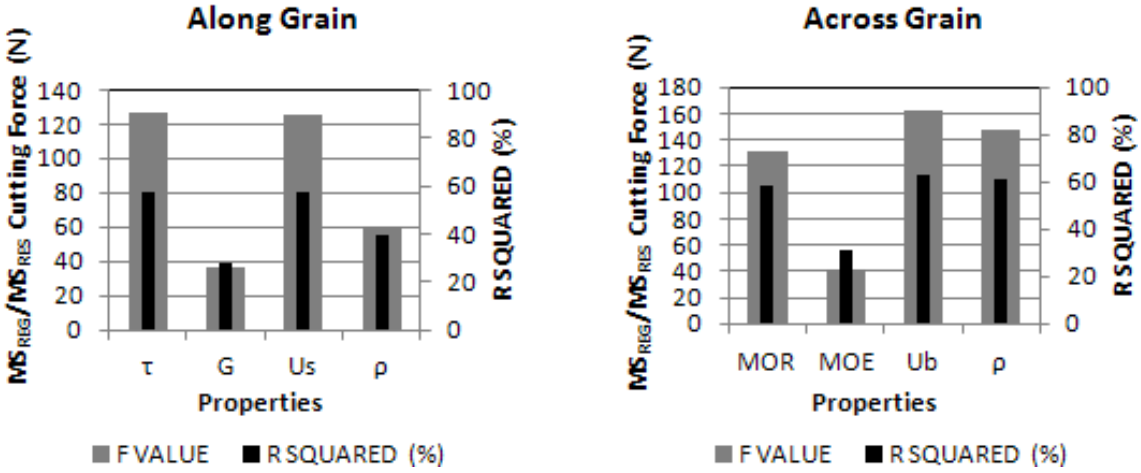

Fig. 7. Significance of the work-piece properties by means of simple least squares

DISCUSSION

Evidence from recently published literature shows regression analyses have been used to develop predictive cutting force models (Axelsson *et al*. 1993; Lhate *et al.* 2011; Porankiewicz *et al*. 2011). These models are mainly focused on the effects of varied tool geometry for band-saw teeth. A linear decrease in the cutting force for an increased positive rake angle (10° to 30°) has been observed (Axelsson *et al*. 1993), whilst at the same time a linear increase in cutting forces is observed for increased edge radii (5 to 20 μm).

The reader should be reminded that the experimental work detailed in this paper used only a simple orthogonal cutting tool with zero rake angle to limit the tool geometry parameters. The rationale behind this is to thoroughly evaluate the effects of work-piece properties for several wood species on the cutting force whilst limiting the tool geometry parameters and cutting conditions. It is furthermore assumed that the effects of edge recession (wear) had no influence on the forces, as the tool was sharpened during regular intervals. Furthermore, the test runs were randomized to remove systematic test run error.

Work-piece parameters have also previously been used as predictors in statistical modelling to describe force trends. The more commonly used parameters are moisture content, grain direction, and density, although coefficients have previously been determined to discretely quantify wood species (Lhate *et al*. 2011). It is generally accepted that tool forces decrease with increased work-piece moisture content. An exception to this rule is for frozen wood specimens (Porankiewicz *et al*. 2011). Furthermore, cutting the wood end grain yields the largest cutting forces, with the lowest cutting forces observed machining along the fibre direction. In general, higher tool forces are observed when cutting wood species of greater density (Lhate *et al*. 2011; Porankiewicz *et al*. 2011). Eyma *et al*. (2004) concluded that density alone acted as a poor work-piece parameter and that mechanical properties need to be utilised in order to develop more accurate cutting force relationships.

The analysis from this study shows that density is weighted as a much better categorical predictor across the grain compared to along the grain. This is by means of higher **F** and $\mathbf{R^2}$ values across the grain (Fig. 7). The obtained strength properties (**MOR, τ**) and toughness (**Ub, Us**) are more consistent as categorical predictors. Coefficients were not calculated to represent the individual wood species tested. The logic behind this decision was to keep the regression models universal, *i.e.* independent of species. The cutting force can be predicted based upon the work-piece mechanical properties, density, and moisture content instead. This model proves that the intrinsic properties of the differing wood species have little influence on the cutting force when each species has been evaluated using a series of carefully obtained mechanical properties.

After using the $\mathbf{R^2}$ and **F** values to determine the effects of each of the mechanical properties on cutting force, **MOE** was removed to re-predict the cutting force across the grain. This did not improve the regression model, and it only reduced the $\mathbf{R^2}$ value by 4%. Likewise, **G** and **ρ** were separately removed to re-predict two separate models. Also, **G** and **ρ** were removed simultaneously to re-predict an additional model. This once again did not improve the original $\mathbf{R^2}$ value, but a decrease up to 1.4% was observed. These results confirm that the accuracy of cutting force prediction is not significantly influenced by **MOE** across the grain and **G** combined with **ρ** along the grain.

The predictive model across the grain has an $\mathbf{R^2}$ value of 90% compared to 80% along the grain. The strength and toughness of the wood have consistently proven to be good predictors and the elastic properties have consistently proven to be poor predictors. Density is not consistent as it proves to be a good predictor along the grain and a poor predictor across the grain. The purpose of machining the radial wood plane was to engage the tool with approximately the same proportion of earlywood and latewood fibres. This was easily achieved across the grain as the tool path is perpendicular to the fibre direction. This was not so easily controlled along the grain. In most cases the radial grain pitch was larger than the 1 mm cutting edge making it extremely difficult to plan a tool path that engages the tool with both the less dense earlywood and denser latewood fibres. This leaves the author with three assumptions:

1. The tool passed through the earlywood fibres only
2. The tool passed through the latewood fibres only
3. The tool passed through a combination of both that cannot be confidently quantified

Regardless which of the assumptions is true, this situation explains why the density acts as a poor predictor along the grain resulting in a lower R^2 value for the respective model.

CONCLUSION

1. The regression models establish novel relationships between the bending properties and cutting forces across the grain and between the shear properties and cutting forces along the grain.
2. The models are completely species independent, *i.e.* no coefficients for species were factored into the models. Only the obtained mechanical properties of the individual wood species were used.
3. Strength (**MOR, τ**) and toughness (**Ub, Us**) have a strong influence on the cutting force both along and across the grain. This has been proven by weighting the categorical predictors used in the regression models.
4. The elastic properties (**MOE, G**) have a weak influence on the cutting force both along and across the grain.
5. **ρ** has a stronger influence on the cutting force across the grain than along. This is evident from the simple least squares analysis and can explain the lower $\mathbf{R^2}$ value and hence more disperse residual plots for the model cutting along the grain.

REFERENCES

ASTM, (2009). "D143-09: Standard test methods for small clear specimens of timber," Pennsylvania.

Axelsson, B., Grundberg, S., and Grönlund, J. (1991). "The use of gray scale images when evaluating disturbances in cutting force due to changes in wood structure and tool shape," *European Journal of Wood and Wood Products* 49, 491-494.

Axelsson, B., Lundberg, Å., and Grönlund, J. (1993). "Studies of the main cutting force at and near a cutting edge," *European Journal of Wood and Wood Products* 51, 43-48.

Cristovao, L., Broman, O., Grönlund, A., Ekevad, M., and Sitoe, R. (2011). "Main cutting force models for two species of tropical wood," Proceedings of the 20th International Wood Machining Seminar, June 7-10, Skellefteå, Sweden.

Eyma, F., Méausoone, P., Martin, P. (2004) "Study of the properties of thirteen tropical wood species to improve the prediction of cutting forces in mode B," *Ann. For. Sci.* 61, 55-64.

Eyma, F., Méausoone., Larricq, P., and Marchal, R. (2005). "Utilization of a dynamometric pendulum to estimate cutting forces involved during routing. Comparison with actual calculated values," *Ann. For. Sci.* 62, 441-447.

Franz, N. C. (1955). "An analysis of chip formation in wood machining," *Forest Products Journal* 10, 332-336.

Franz, N. C. (1958). *An Analysis of the Wood-Cutting Process*, University of Michigan Press, Ann Arbor.

Lhate, I., Cristóvão, L., Ekevad, M., and Sitoe, R. (2011). "Cutting forces for wood of lesser used speceis from Mozambique," in 20th International Wood Machining Seminar, Skellefteå, Sweden.

Loehnertz, S. and Cooz, I. (1998). "Sawtooth forces in cutting tropical hardwoods native to South America," *FPL – RP* – 567, 16 pp.

McKenzie, W. M. (1961). "Fundamental analysis of the wood cutting process," Department of Wood Technology, University of Michigan.

Naylor, A., Hackney, P., and Clahr, E. (2011). "Machining of wood using a rip tooth: Effects of work-piece variations on cutting mechanics," Proceedings of the 20th International Wood Machining Seminar, June 7-10, Skellefteå, Sweden.

Orlowski, K., and Palubicki, B. (2009). "Recent progress in research on the cutting processes of wood. A review," *Holzforschung.* 63, 181-185.

Orlowski, K., Ochrymiuk, T., and Atkins, A. (2011). "Application of mechanics for energetic effects predictions while sawing," Proceedings of the 20th International Wood Machining Seminar June 7-10, Skellefteå, Sweden.

Porankiewicz, B., Axelsson, B., Grönlund, A., and Marklund, B. (2011). "Main and normal cutting forces by machining wood of *Pinus sylvestris*," *BioResources* 6, 3687-3713.

Woodson, G. E., and Koch, P. (1970). "Tool forces and chip formation in orthogonal cutting of loblolly pine," U.S. Department of Agriculture, Forest Service, Southern Forest Experiment Station, New Orleans, LA.

Article submitted: March 13, 2012; Peer review completed: May 8, 2012; Revised version received and accepted: May 18, 2012; Published: May 22, 2012.